International Journal of Concrete Structures and Materials
Vol.18, No.1E, pp.55~61, June 2006

Evaluation and Improvement of Deformation Capacities of Shear Walls Using Displacement-Based Seismic Design

Young-Hun Oh,[1] Sang-Whan Han,[2] and Yeoh-Soo Choi[3]

(Originally published in Korean version of ***Journal of KCI***, Vol.11, No.6, December 1999)

Abstract: RC shear walls are frequently used as lateral force-resisting system in building construction because they have sufficient stiffness and strength against damage and collapse. If RC shear walls are properly designed and proportioned, these walls can also behave as ductile flexural members like cantilevered beams. To achieve this goal, the designer should provide adequate strength and deformation capacity of shear walls corresponding to the anticipated deformation level. In this study, the level of demands for deformation of shear walls was investigated using a displacement-based design approach. Also, deformation capacities of shear walls are evaluated through laboratory tests of shear walls with specific transverse confinement widely used in Korea. Four full-scale wall specimens with different wall boundary details and cross-sections were constructed for the experiment. The displacement-based design approach could be used to determine the deformation demands and capacities depending on the aspect ratio, ratio of wall area to floor plan area, flexural reinforcement ratio, and axial load ratio. Also, the specific boundary detailing for shear wall can be applied to enhance the deformation capacity of the shear wall.

Keywords: shear walls, seismic design, displacement, drift ratio, boundary details.

1. Introduction

Shear wall system is often used for resisting the lateral forces induced by seismic excitation. Since shear walls have relatively high stiffness, they can be used for the lateral force resisting system. Shear wall system can be used effectively for controlling the lateral drift against seismic and wind loads. Most highrise apartment buildings in Korea use shear walls as shown in Fig. 1 for this reason. However, the details of the shear walls used in apartment buildings are different from those of the shear walls used in the United Sates. The shape of the wall used in Korea is rectangular with U-stirrups and cross-ties at the boundaries of the wall.

Previous researches[1-3] reported that the main variables affecting wall details were the ratio of the wall cross-sectional area to the floor-plan area, the wall aspect ratio, the wall axial load, and the wall reinforcement ratios. Therefore, wall details should be related directly to the building configuration. In other words, changes in building configuration lead to changes in wall boundary transverse reinforcement. Meanwhile, multi-story apartment buildings have widely been constructed with shear walls in moderate to high seismic regions. However, there are some differences in the details of these shear walls. The cross-section of the walls used in the United States is barbell-shaped in most cases, while the rectangular cross-section is more common in Korea.

[1] KCI member, Dept. of Architectural Engineering, Konyang University, Nonsan 320-711, Korea.
[2] KCI member, Dept. of Architectural Engineering, Hanyang University, Seoul 133-791, Korea. *E-mail: swhan@hanyang.ac.kr*;
[3] Dept. of Architectural Engineering, Hanyang University, Seoul 133-791, Korea.

The criteria for the structural performance of a shear wall can be represented by the stiffness, strength and deformation capacity inherent in the structure. These capacities are dependent on the load history, sectional shape, vertical and horizontal reinforcement, boundary details, moment to shear ratio, axial load, and concrete strength, etc. The objective of this study is to evaluate the structural performance of slender shear walls having different details with the aspect ratio of two. Specially, this study focuses on the evaluation of the performance of walls with U-stirrups and cross-ties distributed at the boundaries.

To meet the research purpose of this study, four different specimens, which have different boundary details and cross-sections, were constructed and tested. Based on the experimental results, the deformation capacity of shear walls with different cross-sections and boundary details is investigated.

2. Displacement demand and boundary details of shear walls

If the behavior of shear walls was governed by flexure, the

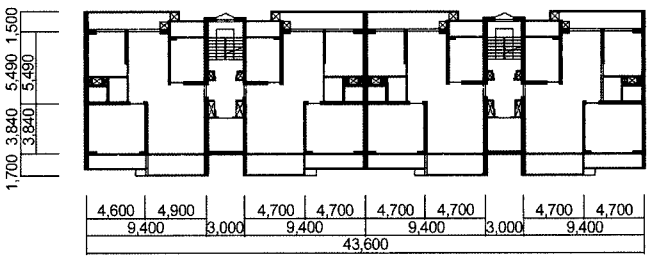

Typical Wall Thickness = 200 (150) mm (unit=mm)

Fig. 1 Typical floor plan for an apartment building in Korea.

fundamental period of a building with shear walls can be estimated by the idealization of an equivalent cantilever.[4] The following equation estimates the fundamental period of vibration from shear wall buildings, where the shear walls have uniform cross-section and carry regularly distributed gravity loads.

$$T = 6.2\frac{h_w}{l_w}n\sqrt{\frac{wh_s}{gE_c\rho}} \tag{1}$$

where, h_w = height of wall, lw = length of wall, n = number of stories, w = unit floor weight including tributary wall weight, h_s = mean story height, g = acceleration of gravity, E_c = modulus of elasticity for concrete, and ρ = ratio of wall area to floor plan area in the direction of consideration.

Based on this formulation, the fundamental period of shear wall buildings can be expressed in terms of the wall aspect ratio, number of stories, and the ratio of wall area to floor plan area.[1,3] The displacement demand for a shear wall building during a major earthquake can be evaluated using the generalized response spectra, such as those presented in Uniform Building Code.[5] The maximum roof displacement (S_d) of a shear wall building can be estimated as follows:

$$S_d = \frac{1.25ZST_{cr}g}{4\pi^2} \tag{2}$$

where, S = soil factor, Z = zone factor, $T_{cr} = \sqrt{2}T$ ($\sqrt{2}$ is used with the assumption that the cracked stiffness is equal to one half of the gross section).

The displacement response as represented by Eq. (2) is based on the single-degree-of-freedom system. Thus, these values can conservatively be multiplied by a factor of 1.5 to estimate the maximum displacement at the roof level of an equivalent multi-degree-of-freedom system.[6] Assuming typical values of w = 8.4 kN/m,^{2} h_s = 2.7 m, E_c = 24100 MPa, Z = 0.4 and S = 1.2 (for firm soil sites) in Eqs. (1) and (2), the mean drift ratio δ_u/h_w) can be expressed as follows;

$$\frac{\delta_u}{h_w} = \frac{1}{4450}\frac{h_w}{l_w}\sqrt{\frac{1}{\rho}} \tag{3}$$

where, δ_u is mean drift, ρ is the ratio of wall area to floor plan area, h_w is height of wall, l_w is length of wall.

The mean drift ratios for various aspect ratios of a wall are plotted as a function of the ratio of wall area to floor plan area in Fig. 2. The displacement demand is sensitive to the ratio of wall area to floor plan area in the direction of consideration. For U.S. buildings, the ratio of wall to floor area is about 0.5~1%.[1,2] Meanwhile, typical Korean residential buildings are mostly constructed using shear wall system for lateral load resistance where ratios of wall to floor area of 2~3.5% are common. The displacement demand for typical buildings in America exceeded 1% of drift ratio for all walls with aspect ratios greater than 3. The displacement demand for Korean buildings was less than 1.2% of the drift ratio for walls with aspect ratios of up to 7. The maximum drift demand of a shear wall building subjected to major earthquakes may range from 1.2% of drift ratio in Korean buildings to 1.5~2% of drift ratio in the U.S. buildings. Therefore, it is necessary to evaluate the deformation capacities of shear walls with different boundary details and ratios of wall to floor area.

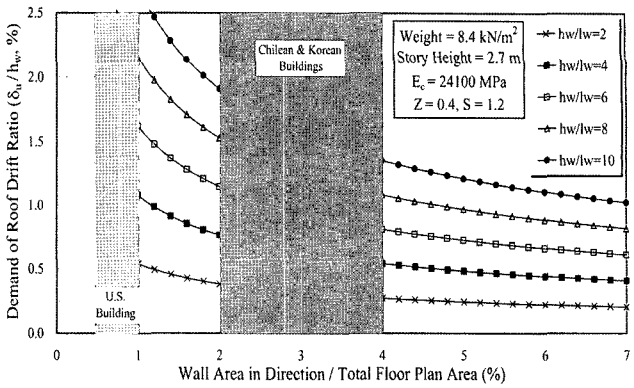

Fig. 2 Displacement demand for a shear wall system.

Inelastic energy dissipation is normally concentrated in critical regions at the base of walls. Critical regions of shear walls should be proportioned and detailed to resist repetitive cyclic inelastic deformation without significant degradation in shear strength. According to the ACI code,[7] shear walls require confined boundary elements whenever the calculated compressive stress exceeds $0.2f'_{ck}$ under the factored loading. The boundary elements must be capable of resisting gravity loads and overturning moments induced by the earthquake without the contribution of the wall web. Those boundary elements are essentially same as columns placed at the compression region of wall and have transverse reinforcement at least equal to that required in column critical regions. The confinement at the wall boundary must be continued through the height of the wall until the extreme fiber stress is less than $0.15f'_{ck}$.

The longitudinal reinforcement is usually concentrated at the edge. The requirements for the wall web reinforcement in the United States and Korea are similar; The United States and Korean codes[8] require a minimum of 0.25% horizontal and vertical reinforcement.

In this study, transverse reinforcement details at the boundary elements were basically proportioned to satisfy the requirements of the transverse reinforcement for a column. Although transverse reinforcement at a boundary element consisted of both U-stirrups and cross-ties, the spacing was determined so that it would not exceed 16 times longitudinal bar diameters ($16d_f$), 48 times transverse reinforcement diameter ($48d_f$), or the least dimension of the boundary element. U-stirrups were fabricated to accommodate the development length greater than 20 times the transverse reinforcement diameter ($20d_f$). Cross-ties having 135° and 90° hooks at the ends were prepared to have the development length of at least 6 times greater the transverse reinforcement diameter ($6d_f$).

3. Experimental program

3.1 Details of shear wall specimens

The prototype structure shown in Fig. 1 is a fifteen-story reinforced concrete shear wall building located in Korea. It was designed by the specifications of the Building Code for Reinforced Concrete[8] and the Standard Design Loads for Buildings[9] with a seismic force reduction factor R of 3.5. Although some parameters for calculating seismic design force by Korean seismic provision would slightly differ from UBC-94 and ATC 3-06,[10] the seismic design force for the shear wall system of Korean

buildings range between those of UBC-94 and ATC 3-06 in a setting of moderate seismic region. The requirements for designing structural elements including the walls are similar to ACI 318-95. Actual aspect ratios of shear walls in the proto-type building ranged from 4.5 in the transverse direction to 7.0 in the longitudinal direction, but moment-to-shear depth ratios ($M_u / V_u \cdot d$), which were calculated for major walls in both directions using linear static and time history analysis of three dimensional modeling of the proto-type building, ranged from 1.5 to 3.5 as shown in Fig. 3. It is construed that the difference between physical and calculated aspect ratios was attributed to the higher vibration modal characteristics of the proto-type building. Thus, the aspect ratio of wall specimens in the experimental program was set to 2.

Four full-scale wall specimens were made. All four specimens had the same overall dimensions of 3000 mm in height and 1,500 mm in the width. The thickness of three specimens was 200 mm. However, the barbell-shaped specimen (HRI-W7) had a wall web with a thickness of 125 mm, and the boundary columns at its edges had a cross section of 240 mm × 240 mm. The dimensions and reinforcement details of each specimen are shown in Table 1 and Fig. 4. The HRI-W2 specimen was the control specimen, reproducing the common practices used for residential buildings in Korea. Its boundary elements were confined to D10 (A_s = 71 mm^2) U-stirrups and cross-ties spaced at 200 mm. The HRI-W5 specimen had the same dimensions and reinforcement details except for the U-stirrups and cross-ties at the boundary elements spaced apart at 100 mm. This specimen was made to evaluate the effect of the spacing of the U-stirrups and cross-ties at the boundary element on its overall response. The HRI-W7 and HRI-W8 specimens of barbell- and T-shaped cross-section, respectively, were prepared to compare the results with those of HRI-W2 specimen of rectangular cross-section.

3.2 Material properties

Ready mixed concrete with 19 mm maximum aggregate was used. The average compressive strength for each concrete specimen was in the range of 29.4-31.8 MPa at 28 days and 32.9-36.2 MPa at the test date. The average reinforcement strengths were f_y = 342 MPa (f_u = 445 MPa) for D10 reinforcing bar, and f_y = 449 MPa (f_u = 617 MPa) for D13 reinforcing bar. More

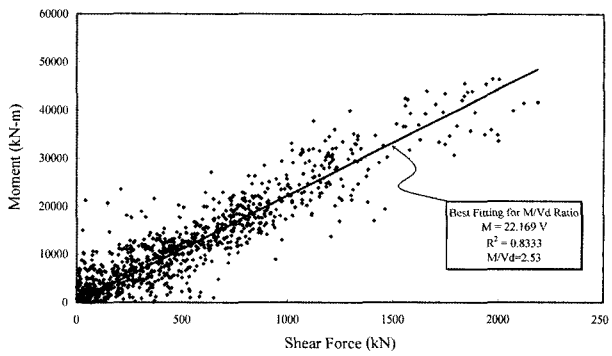

Fig. 3 Moment vs. shear ratios for a shear wall system.

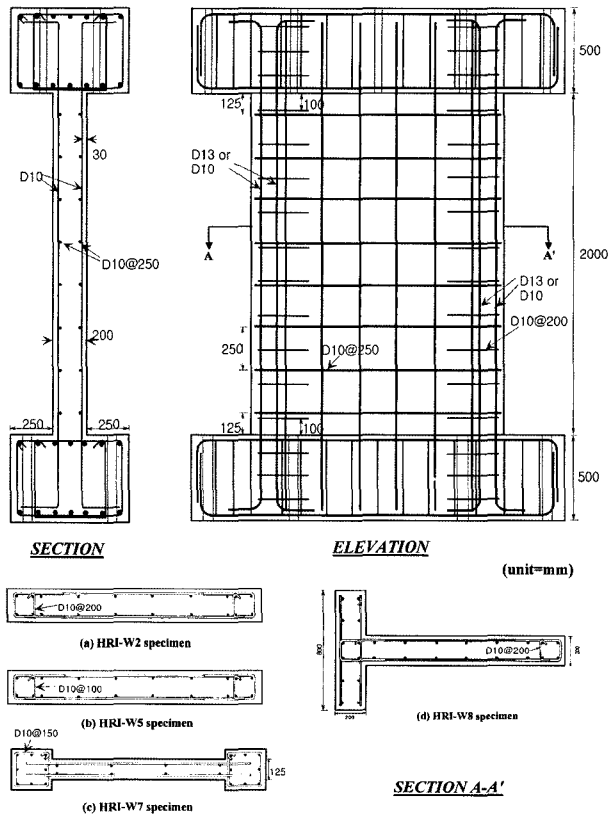

Fig. 4 Configuration of shear wall specimens.

Table 1 Dimension and reinforcement details of experimental specimens (length unit = mm).

Specimen	Cross section and details	Aspect ratio	Axial stress ($N/A_g f'_{ck}$)	f'_{ck} [1](MPa)	ρ_b [2](%)	ρ_h [3](%)	ρ_v [4](%)	ρ_s [5](%)
HRI-W2	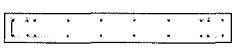	2.0	0.10	27.6	4-D13 (1.27)	D10@250 (0.28)	D10@220 (0.32)	D10@200 (0.99)
HRI-W5	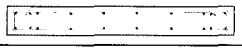	2.0	0.10	27.6	4-D13 (1.27)	D10@250 (0.28)	D10@220 (0.32)	D10@100 (1.97)
HRI-W7	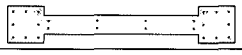	2.0	0.10	27.6	8-D10 (0.99)	D10@400 (0.28)	D10@320 (0.36)	D10@150 (0.94)
HRI-W8	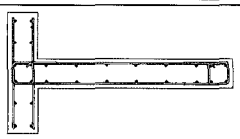	2.0	0.10	27.6	4-D13 (1.27)	D10@250 (0.28)	D10@220 (0.32)	D10@200 (0.99)

[1] Design compressive strength of concrete
[2] The ratio of boundary longitudinal reinforcement to boundary element area
[3] The ratio of web horizontal reinforcement to vertical cross section
[4] The ratio of web vertical reinforcement to horizontal cross section
[5] The volumetric ratio of transverse reinforcement at the boundary element

information can be provided by the authors.[11, 12]

3.3 Test setup and procedure

The specimens were bolted to a firm floor and tested in a vertical position. To ensure out-of-plane stability, two steel frames were placed perpendicular to the specimen. Fig. 5 shows the test setup that can vary the moment-to-shear ratios ($M_u/V_u \cdot d$). This is feasible when two vertical actuators are controlled to exert an axial force to produce additional moment in addition to a vertical axial force. However, since the moment-to-shear ratio was set to 2 in this study, it did not require the exertion of additional moment by the two vertical actuators.

The instrumentation included load cells to measure various forces, electrical resistance strain gauges to measure strains, and linear variable differential transducers (LVDTs) to measure flexure and slippage deformations of each test specimen. Readings from the load cells, electrical resistance strain gauges and LVDTs were continually recorded by a data acquisition system.

A vertical load of $0.1f'_c A_g$ was applied to the specimens at the beginning of each test and throughout the test. This level of vertical load was to represent the action of dead load in the prototype building. The amount of axial load was well below the calculated balanced axial load for the wall specimens.

Cyclic lateral load was applied to the load transfer assembly on the top of the specimen through a hydraulic actuator attached to the reaction wall, which operated in a displacement-controlled manner. The top displacements were cycled three times to increasing levels of drift ratios (top displacement divided by height) as shown in Fig. 6. The drift ratios were approximately 1/600, 1/400/, 1/300, 1/200, 1/150, and 1/33.

4. Experimental results

4.1 Cracks and failure modes

When the lateral load of 129.4~215.6 kN, which was developed at the drift ratio of 1/600~1/400 (0.17~0.25%), was applied, initial flexural cracks in the specimens occurred at the lower part of the tensile zone. After that, a large number of flexural cracks occurred at the drift ratio of 1/300 (0.33%), and these cracks progressed into flexural-shear cracks at the drift ratio of 1/200 (0.5%). As the drift ratio increased, new cracks developed at the upper parts of all

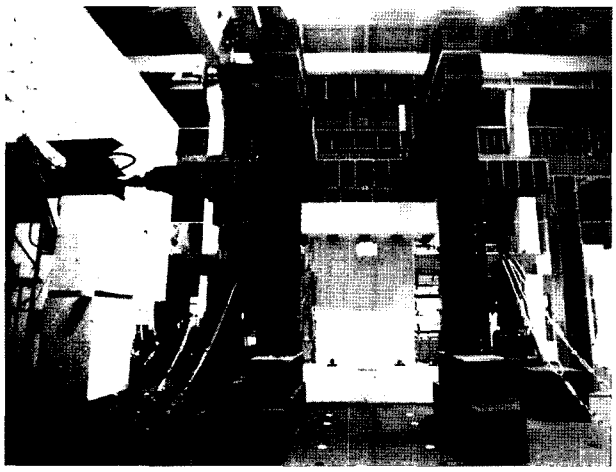

Fig. 5 Test setup.

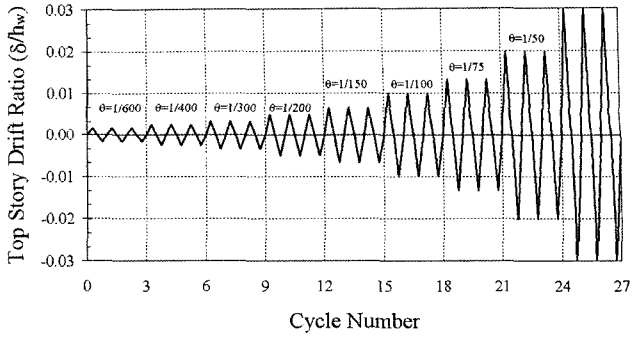

Fig. 6 Applied displacement history.

specimens.

Although HRI-W2, HRI-W5, and HRI-W7 specimens generally behaved in a flexural manner by yielding due to the longitudinal reinforcement and suppressing of a premature shear failure, these specimens failed finally due to the buckling of longitudinal reinforcement and/or crushing of the concrete at the compression zone of the boundary elements beyond the drift ratio of 1/50 (2%). However, as for negative loading, when the flange was under tension, HRI-W8 specimen experienced crushing of the concrete and buckling of the vertical reinforcement at the lower part of the wall web. This caused the final failure of the specimen. On the other hand, the lower part of the flange exhibited neither concrete crushing nor buckling of the vertical reinforcement. The crack propagation and final failure mode are shown in Fig. 7. In this figure, cracks are marked as dotted lines in the grid line representing the spacing of the reinforcement, and hatched areas represent the splitting region of the concrete specimen.

4.2 Loads vs. deformation characteristics

All four specimens experienced yielding at the drift ratio of 1/250~1/300 All the specimens showed gradually increasing lateral load carrying capacity up to the drift ratio of approximately 1.5%. At this deformation level, these specimens exhibited their maximum strength and maintained ductile behavior without any loss of lateral load carrying capacity. The plots of load vs. deformation are shown in Fig. 8.

The important values for the load vs. deformation relationship are shown in the inset box in Fig. 8. Displacement and ductility capacity were measured when the applied load was reduced by 20% of maximum strength. Yield displacements were measured when all longitudinal bars at the end (10% of l_w) have yielded. The ductility ratio was computed as the ratio of the maximum displacement divided by the yield displacement.

Table 2 shows the strength and deformation characteristics of each specimen. Consequently, the deformation capacities were evaluated by means of the ductility ratio and the drift ratio. In Table 2, the calculated maximum strengths ($V_{max(cal)}$) were determined as the minimum value between nominal shear strength specified by ACI 318-95 and shear force corresponding to the maximum flexural strength obtained from sectional analysis. Flexural strengths were calculated by assuming a linear strain distribution across the section and a peak compressive strain of 0.003 in the concrete. Strain hardening of the longitudinal reinforcement was also considered. Because the distribution of the lateral forces over the height of the wall was unique, the shear force at the base

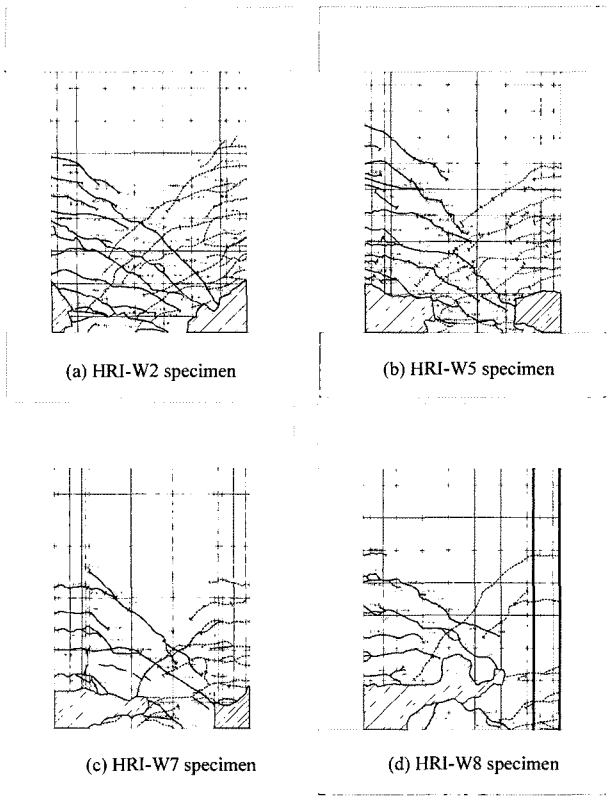

Fig. 7 Crack pattern at the final loading.

corresponding to the maximum flexural strength could be calculated. For all specimens, maximum strengths were governed by the shear force corresponding to the maximum flexural strength obtained from sectional analysis. Also, these values corresponded well with the observed maximum strength of each specimen.

According to Fig. 8 and Table 2, every specimen had a deformation capacity larger than 1.5% and a displacement ductility ratio larger than 3.0.

5. Comparison of structural performance of shear wall specimens

The control specimen, HRI-W2, showed that the ductility ratio was 6.5, and the drift ratio was 2.7% of the wall height under positive loading, and 1.8% under negative loading. Specimen HRI-W5 displayed better ductile behavior than the control specimen, HRI-W2. It had ductility ratios of 9.2 and 8.9, and drift ratios of 2.9% and 2.8% for the positive and negative loading direction, respectively. The barbell-shaped specimen, HRI-W7, had ductility ratios of 7.7 and 5.4 and drift ratios of 2.8% and 1.8%. The T-shaped specimen, HRI-W8, had ductility ratios of 10.0 and 5.2, and drift ratios of 1.9% and 1.7% for the positive and negative loading direction, respectively.

It was observed that the specimens of rectangular cross-section displayed equivalent or greater deformation capacities compared to those of the barbell-shaped HRI-W7 specimen. The response patterns of the specimens of rectangular cross-section, HRI-W2 and HRI-W5, might be attributed to the content of wall boundary confinement. As shown in Fig. 9 through Fig. 12, specimen HRI-W5 displays the most ductility in both loading directions among all specimens. In these figures, each parameter for evaluating the structural performance is compared with the volumetric ratio of the wall boundary confinement.

It is construed that all specimens might have deformation capacities greater than drift ratio of 1.5%. The ductility ratios for all specimens exceeded 3.0.

Fig. 12 shows the energy dissipation capacity, which is calculated from the load-displacement curve and is also normalized by the product of yield strength and yield displacement,

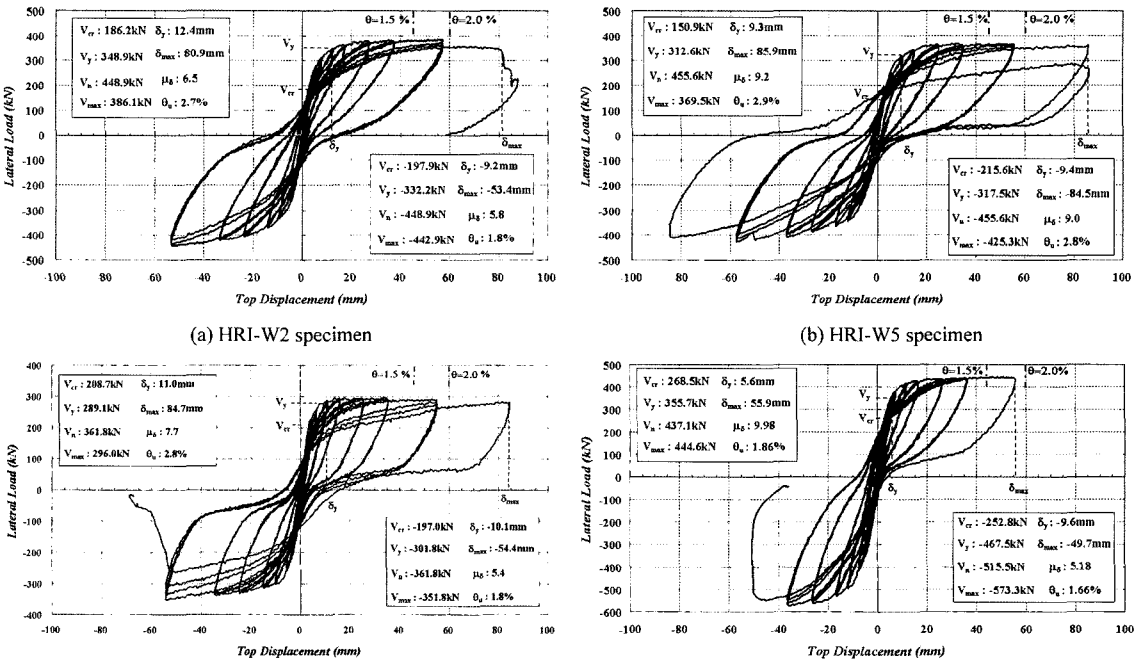

Fig. 8 Load versus displacement relationship of each test specimen.

Table 2 Observed strength and deformation capacity of shear wall specimens.

Specimen	Loading direction	f_c [1] (MPa)	V_{cr} [2] (kN)	V_y [3] (kN)	$V_{max(test)}$ [4] (kN)	$V_{max(cal)}$ [5] (kN)	$\frac{V_{max(test)}}{V_{max(cal)}}$ [6]	δ_y [8] (mm)	δ_{max} [9] (mm)	μ_δ [10]	θ_u [11] (%)
HRI-W2	Positive	34.2	186.2	348.9	386.1	378.3	1.02	12.4	80.9	6.5	2.7
	Negative	(29.4)	198.0	332.2	442.9		1.18	9.2	53.4	5.8	1.8
HRI-W5	Positive	36.2	150.9	312.6	369.5	378.3	0.98	9.3	85.9	9.2	2.9
	Negative	(30.3)	215.6	317.5	425.3		1.13	9.4	84.5	8.9	2.8
HRI-W7	Positive	33.7	208.7	289.1	296.0	337.1	0.88	11.0	84.7	7.7	2.8
	Negative	(31.8)	197.0	301.8	351.8		1.04	10.1	54.4	5.4	1.8
HRI-W8	Positive	34.5	268.5	355.7	446.6	501.8	0.89	5.6	55.9	10.0	1.9
	Negative	(28.6)	252.8	467.5	573.3	544.9	1.05	9.6	49.7	5.2	1.7

[1] Compressive strength of the concrete specimen at test day (and at 28th day)
[2] Observed shear force at first cracking
[3] Observed shear strength when all boundary longitudinal reinforcements yield
[4] Maximum observed strength during the test
[5] Maximum strength calculated as the minimum value between nominal shear strength specified by ACI 318-95 and shear force corresponding to maximum flexural strength obtained from sectional analysis
[6] The ratio of maximum observed shear strength to maximum calculated strength
[7] Displacement when all boundary longitudinal reinforcements yield
[8] Displacement corresponding to 80 percent of the maximum strength
[9] Displacement ductility calculated from dividing the maximum displacement by the yield displacement
[10] Drift ratio calculated from dividing the maximum displacement by the wall height

for each specimen. The energy dissipation capacity of three specimens except for the T-shaped HRI-W8 specimen exhibited almost a similar trend until the 21st cycle (drift ratio of 1/50). The rate of increase in energy dissipation accelerated with increasing top drift ratios. Beyond the drift ratio of 1/50, the specimen HRI-W5 with closely spaced transverse reinforcement at the boundary elements displayed a large increase in energy as shown in Fig. 12. HRI-W8 specimen had the most superior energy dissipation capacity because its flexural strength and stiffness were greater than the other three specimens due to the contribution of flanged section. However, the excellent energy dissipation capacity of the HRI-W8 specimen was restrained by crushing at the compression zone in the wall web, which showed limited deformability at the drift ratio of 1.7%.

Additionally, HRI-W2 specimen serving as a control specimen displayed an almost equivalent energy dissipation capacity compared with the barbell-shaped sectional specimen of HRI-W7.

It is construed that the content of transverse reinforcement in the rectangular specimens could play an important role in the ductile hysteretic response. Finally, all specimens showed desirable behavior and had sufficient deformation capacity compared to the estimated deformation demand as indicated in the previous section.

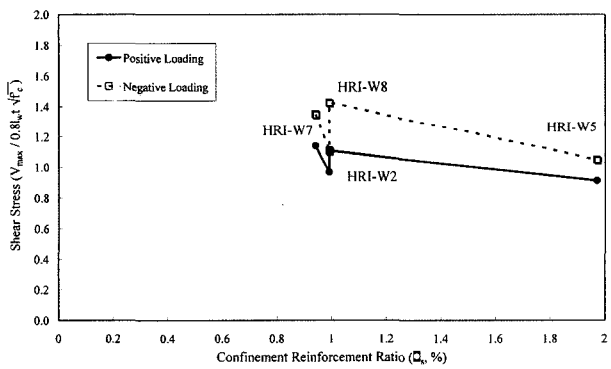

Fig. 9 Average shear stress at the maximum strength.

6. Conclusions

This study investigated the seismic behavior of shear walls of different details and cross-sections. An experimental study was

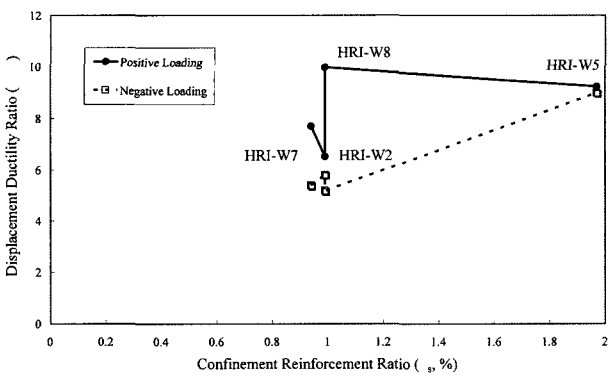

Fig. 10 Comparison of drift ratios of specimens.

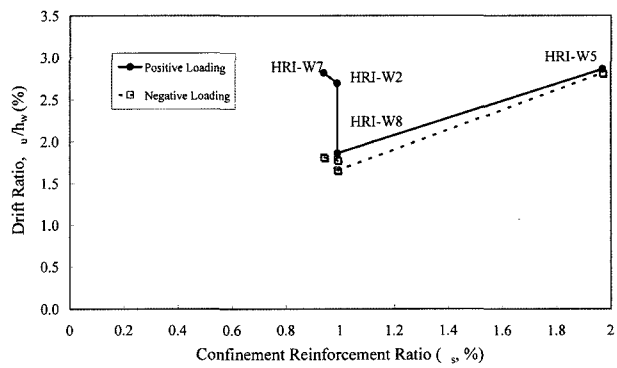

Fig. 11 Displacement ductility ratios of specimens.

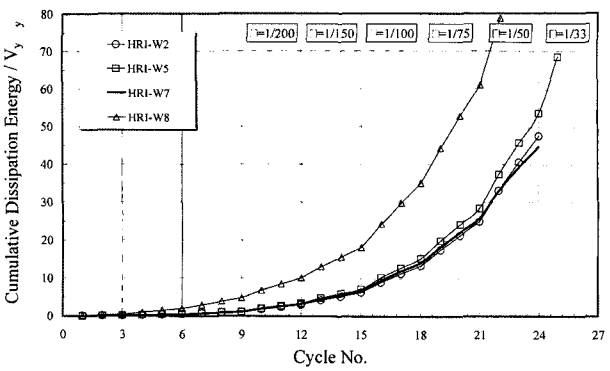

Fig. 12 Normalized energy dissipation of specimens Normalized energy dissipation of specimens.

carried out for this purpose. Four full-scale wall specimens were made. On the basis of the results obtained from this study, the following conclusions were drawn.

1) Failure in all specimens occurred at last due to the crushing of the concrete at the lower parts of boundary elements. However, only HRI-W2R specimens failed due to not only the crushing of the concrete but also the bar buckling.

2) All specimens have ductility and deformation capacities greater than 3.0 and 1.5% of height, respectively. Thus, the walls considered in this study had satisfactory deformation and ductility capacities compared to the values specified in the design provision[9] and the deformation demand computed by displacement-based design approach.

3) The transverse reinforcement of boundary element in shear walls, which satisfied the code of minimum transverse reinforcement in tied column, was found that it could confine the concrete at the boundary region of the shear wall, while it should resist both the compressive force as found on the bottom floor of wall system apartment and the overturning moment induced by lateral force.

4) The HRI-W5 and HRI-W7 Specimens, which were prepared to investigate the structural performance of various sectional shapes of the walls, exhibited nearly equal experimental results in terms of ductility ratio, drift ratio, and energy dissipation capacity.

5) Specimens of HRI-W7 and HRI-W8 were intended to investigate the structural capacity according to the sectional shapes of the walls and showed the results, which satisfied the deformability in accordance with the deformation demand.

6) It is construed that the transverse reinforcement in the form of U-stirrups and cross-ties provides confinement to the core concrete in the boundary elements of the shear walls. It is expected that such boundary element details can provide a feasible solution to effectively confine the boundary elements of rectangular walls, which are widely used in the construction of residential buildings in some countries because of their economic advantage.

Acknowledgments

This work was supported by a Korea Research Foundation Grant (KRF-2003-003-D00513) and MOST/ERC R11-2005-056-04002-0.

References

1. Wallace, J. W. and Moehle, J. P., "Ductility and Detailing Requirements of Bearing Wall Buildings," *Journal of Structural Eng., ASCE*, Vol.116, 1992, pp.1625~1644.

2. Wood, S. L., Wight, J. K., and Moehle, J. P., *The 1985 Chile Earthquake Observations on Earthquake-resistant Construction in Vina del Mar*, SRS No. 532, Univ. of Illinois, Urbana, Illinois, 1987.

3. Tomsen IV, J. H. and Wallace, J. W., *Displacement-based Design of RC Structural Walls*, Report No. CU/CEE-95/06, Clarkson Univ., New York, 1995.

4. Sozen, M. A., "Earthquake Response of Buildings with Robust Walls," *Proceedings of Fifth Chilean Conference on Seismology and Earthquake Eng., Santiago*, 1989.

5. International Conference of Building Officials (ICBO), *Uniform Building Code*, Whittier, California, 1994.

6. Nassar, A. A. and Krawinkler, H., *Seismic Demands for SDOF and MDOF Systems*, John A. Blume Earthquake Engineering Center, Report No.95, Stanford Univ., 1991.

7. American Concrete Institute (ACI), *Building Code Requirements for Reinforced Concrete and Commentary*, ACI 318-95, Farmington, Michigan, 1995.

8. Ministry of Construction, *Building Code for Reinforced Concrete*, Seoul, Korea, 1994.

9. Ministry of Construction, *Standard Design Loads for Building Construction*, Seoul, Korea, 1992.

10. ATC 3-06, *Tentative Provisions for the Development of Seismic Regulations for Buildings*, Applied Technology Council, Palo Alto, California, 1978.

11. Han, S. W., Oh, Y. H., and Lee, L. H., "Effect of Edge Confinement on Deformation Capacity in the Isolated RC Structural Walls," *Journal of Korea Concrete Institute*, Vol.11, No 6, 1999, pp.101~112. (in Korean)

12. Han, S. W., Oh, Y. H., Oh, C. H., and Lee, L. H., "Structural Performance of Shear wall with Sectional Shape in Wall-type Apartment Buildings," *Journal of Korea Concrete Institute*, Vol.12, No.4, 2000, pp.3~14 (in Korean).